APOLD1 loss causes endothelial dysfunction involving cell junctions, cytoskeletal architecture, and Weibel-Palade bodies, while disrupting hemostasis

Simon Stritt,[1]* Paquita Nurden,[2]* Alan T. Nurden,[2] Jean-François Schved,[3] Jean-Claude Bordet,[4] Maguelonne Roux,[5] Marie-Christine Alessi,[6] David-Alexandre Trégouët,[5,7] Taija Mäkinen[1] and Muriel Giansily-Blaizot[3]

[1]Department of Immunology, Genetics and Pathology, Uppsala University, Uppsala, Sweden; [2]Institut de Rythmologie et de Modélisation Cardiaque, Hôpital Xavier Arnozan, Pessac, France; [3]Department of Biological Hematology, CHU Montpellier, Université de Montpellier, Montpellier, France; [4]Hematology, Hospices Civils de Lyon, Bron Biology Center and Hemostasis-Thrombosis, Lyon-1 University, Lyon, France; [5]Laboratory of Excellence GENMED (Medical Genomics), Paris, France; [6]Aix Marseille University, INSERM, INRAE, C2VN, Marseille, France and [7]University of Bordeaux, INSERM, Bordeaux Population Health Research Center, U1219, Bordeaux, France.

Abstract

Vascular homeostasis is impaired in various diseases thereby contributing to the progression of their underlying pathologies. The endothelial immediate early gene *Apolipoprotein L domain-containing 1* (*APOLD1*) helps to regulate endothelial function. However, its precise role in endothelial cell biology remains unclear. We have localized APOLD1 to endothelial cell contacts and to Weibel-Palade bodies (WPB) where it associates with von Willebrand factor (VWF) tubules. Silencing of *APOLD1* in primary human endothelial cells disrupted the cell junction-cytoskeletal interface, thereby altering endothelial permeability accompanied by spontaneous release of WPB contents. This resulted in an increased presence of WPB cargoes, notably VWF and angiopoietin-2 in the extracellular medium. Autophagy flux, previously recognized as an essential mechanism for the regulated release of WPB, was impaired in the absence of APOLD1. In addition, we report *APOLD1* as a candidate gene for a novel inherited bleeding disorder across three generations of a large family in which an atypical bleeding diathesis was associated with episodic impaired microcirculation. A dominant heterozygous nonsense *APOLD1*:p.R49* variant segregated to affected family members. Compromised vascular integrity resulting from an excess of plasma angiopoietin-2, and locally impaired availability of VWF may explain the unusual clinical profile of *APOLD1*:p.R49* patients. In summary, our findings identify APOLD1 as an important regulator of vascular homeostasis and raise the need to consider testing of endothelial cell function in patients with inherited bleeding disorders without apparent platelet or coagulation defects.

Introduction

Regulation of vascular integrity and the prevention of excessive leakage of blood components are central for homeostasis and ensure proper organ function. Endothelial permeability varies between different vascular beds and is adjusted to the respective tissue functions, thereby allowing for gas exchange, regulation of extracellular fluid volume, osmolarity, pH as well as ion concentration. Breakdown of vascular integrity is a key feature of numerous pathologies including not only acute and chronic inflammatory diseases such as infections, asthma and arthritis, but also cancer and ischemic cardiovascular diseases with emphasis on myocardial infarction and stroke.[1,2]

Vascular barrier function is mainly established by intercellular adherens and tight junctions between adjacent endothelial cells (EC). The abundance and structural organization of junctional proteins such as claudin-5 (CLDN5) or vascular endothelial cadherin (VE-Cad; CDH-5) together with their modulation, spatially and temporally, determine vessel permeability. Stimulation of EC with inflammatory mediators such as thrombin[3] or angiopoietin-2 (ANGPT2)[4] results in EC activation, junction opening and the formation of intercellular gaps. Likewise, vascular injury or ischemia triggers EC activation and the release of bioactive mediators from Weibel-Palade bodies (WPB) such as von Willebrand factor (VWF) and ANGPT2 thereby interfering with coagulation and also vessel permeability.[5–7] In addition, endothelial activation is accom-

panied by the expression of immediate early genes such as *JUN* and *FOS* as well as the more recently identified *Apolipoprotein L domain-containing 1 (APOLD1)*.[8,9] Platelet-, EC- and neuron-restricted APOLD1 has been implicated in angiogenesis as well as the regulation of endothelial permeability in mice in response to transient brain ischemia.[9–12] However, its precise role in EC biology as well as the molecular mechanisms involved remain unclear. Using *in vitro* knockdown studies in human dermal blood EC (HDBEC), we now define a role of APOLD1 in modulating the endothelial cytoskeleton, cell-cell junctions and WPB biology. Transfection of HDBEC with *APOLD1* siRNA resulted in an increased release of WPB through altered autophagy flux in favor of cargo secretion. The findings may also have clinical implications, because an inherited *APOLD1[R49*]* stop codon variant segregated to patients with bleeding of primarily vascular origin within a large French family. Affected family members presented with a severe atypical bleeding diathesis despite unaltered platelet function that has remained undiagnosed during more than 20 years of extensive clinical and biological testing in expert centers including evaluations for platelet, coagulation and connective tissue defects. Treatment of bleeding during delivery or some surgical interventions was complicated not only because platelet transfusions failed to stop blood loss but also because the use of desmopressin to increase VWF secretion from EC provoked a transiently impaired microcirculation. Our study highlights a new molecular pathway that may link defects primarily affecting EC to a bleeding syndrome.

Methods

Cell culture, preparation of platelets,[13] immunolabeling of platelets and HDBEC,[13] immunogold/transmission electron microscopy, immunoblotting, gene silencing, *in vitro* permeability assay, VWF, ANGPT1 and ANGPT2 enzyme-linked immunosorbent assays, image acquisition and image analysis[14,15] were either performed according to the manufacturers' protocols or as previously described and are detailed in the *Online Supplementary Information*.

Whole exome and Sanger sequencing

Whole exome sequencing (described in detail in the *Online Supplementary Information*) identified two candidate variants in a large French family. Of these, *APOLD1*:p.R49* resulting from the combination of a common variant and a rare adjacent nucleotide substitution *in cis*, was a primary nonsense variant. Segregation analysis of both the common c.146G>A variant and the rare c.145C>T substitution in *APOLD1* was performed on DNA from ten family members of three generations by Sanger sequencing. Blood samples were obtained from patients after in-

formed consent in accordance with the Declaration of Helsinki. Ethical approval was obtained in France from INSERM (RBM 04–14) for the national project "Network on the inherited diseases of platelet function and platelet production" and from the Montpellier local ethical committee (N. 202000352) for the project "Identification of new genes involved in platelet abnormal functions".

Data presentation and statistical analysis

Data visualization and statistical testing were performed using GraphPad Prism 7. A nonparametric Wilcoxon-Mann-Whitney test was used for comparisons of two means. For multiple comparisons one-way analysis of variance (ANOVA) followed by a Dunnett multiple comparison test or a two-way ANOVA followed by a Sidak or Tukey multiple comparison test was performed. *P*-values <0.05 were considered as statistically significant: *$P< 0.05$; **$P< 0.01$; ***$P< 0.001$.

Results

APOLD1 localizes to cell-cell junctions and Weibel-Palade bodies

Given the endothelial and megakaryocyte/platelet-restricted expression of APOLD1,[9,11] we first assessed its localization in primary HDBEC and human platelets. In agreement with previous reports, we detected APOLD1 at cell-cell junctions, defined by the presence of VE-Cad, of HDBEC in culture and in addition, we found a co-localization with the major WPB constituent VWF (Figure 1A). The WPB-specific localization of APOLD1 was further confirmed by immunogold electron microscopy (Figure 1B). While an occasional gold particle localized to the external membrane, the majority of gold particles were found inside the WPB suggesting an association of APOLD1 with the tubules of VWF (shown at high magnification in Figure 1B$_{iii}$). Of note, immunofluorescence labeling of platelets from human controls revealed localization of APOLD1 to α-granules and exclusion from δ-granules/lysosomes (*Online Supplementary Figure S1A, B*). Ultrastructurally, APOLD1 was occasionally found associated with the membrane of α-granules (Figure 1C$_{i-iii}$). Immunogold labeling also showed an eccentric localization of APOLD1 in the α-granule lumen (Figure 1C$_{iv}$), a finding previously described by Cramer *et al.*[16] for platelet-stored VWF in a manner resembling WPB.

APOLD1 regulates the junctional and cytoskeletal architecture in endothelial cells

To further study the function of APOLD1, we validated four short interfering RNA (siRNA) for their ability to ablate *APOLD1* expression (*Online Supplementary Figure S2A*). Efficient silencing was confirmed by immunoblotting and immunolabeling (*Online Supplementary Figure S2B, C*).

APOLD1 silencing in HDBEC resulted in similar cellular changes for all tested siRNA *(Online Supplementary Figure S2D)*. These changes were characterized by an increase in cell size as well as altered shape (Figure 2A-D) and were associated with EC junction dismantling, evidenced by a reduction in the tight junction protein CLDN5, platelet-EC adhesion molecule 1 (PECAM1/CD31) as well as the reorganization of VE-Cad-positive adherens junctions (Figure 2A, B, E). Moreover, we also found a markedly enhanced fibronectin fibrillogenesis and actin stress fiber formation, reminiscent of EC activation (Figure 2A, B, E). Functionally, the observed alterations in the absence of APOLD1 resulted in increased endothelial permeability to 40 kDa FITC-dextran, assessed by a transwell permeability assay (Figure 2F). Of note, 50% loss of APOLD1 protein recapitulated the cellular defects observed upon efficient silencing *(Online Supplementary Figures S2C and S3)*.

These results reveal a critical role of APOLD1 in controlling
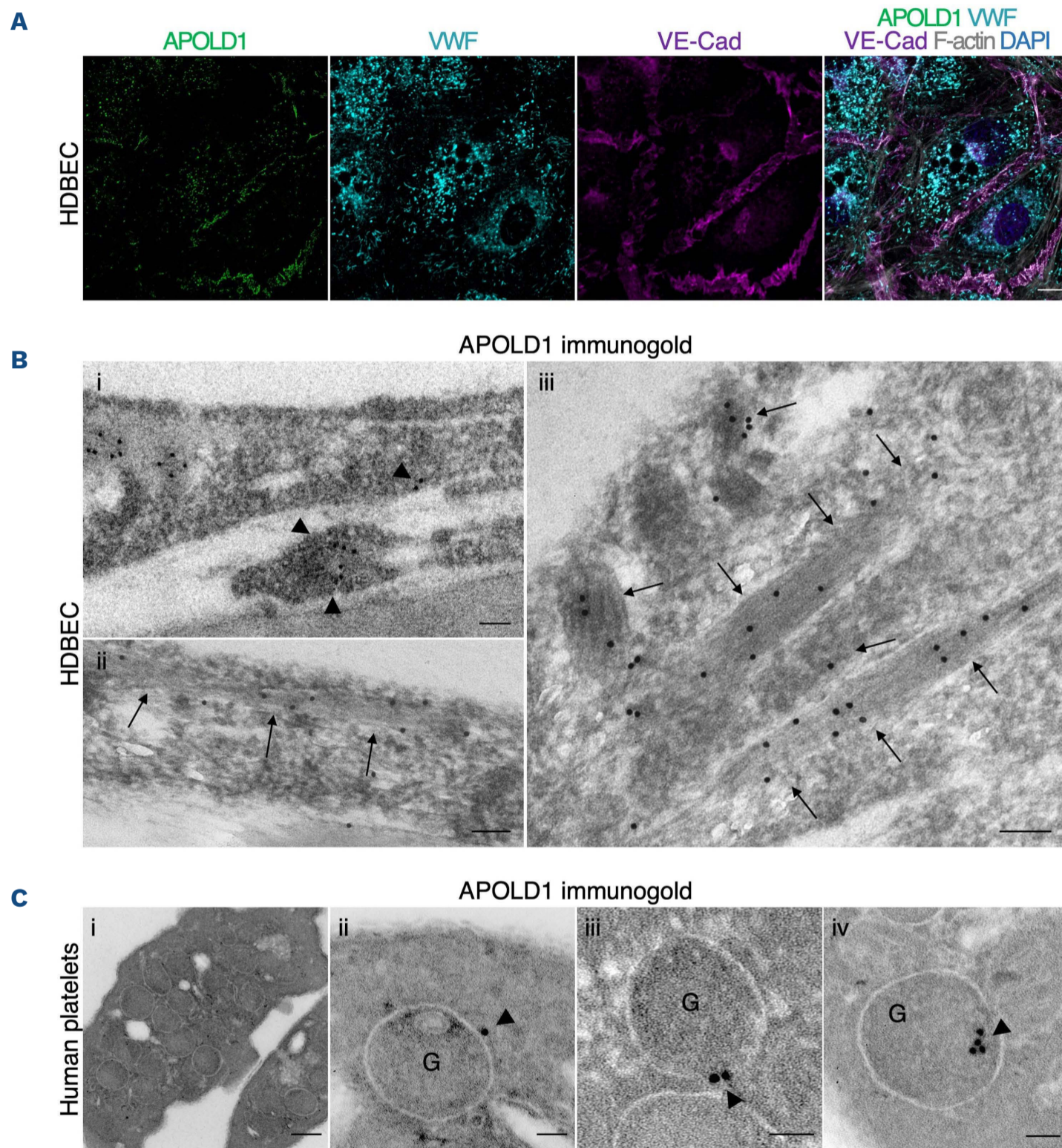
Figure 1. APOLD1 localizes to endothelial cell-cell junctions and von Willebrand factor storage organelles. (A) Cultured human dermal blood endothelial cells (HDBEC) were immunolabeled for Apolipoprotein L domain-containing 1 (APOLD1; green [processed by super-resolution radial fluctuations[52]]), von Willebrand factor (VWF; cyan), vascular endothelial cadherin (VE-Cad; magenta), F-actin (gray), and nuclei were highlighted with DAPI (blue) and subsequently analyzed by confocal microscopy. Scale bar, 10 μm. (B) Immunogold labeling of adherent HDBEC for APOLD1 and subsequent electron microscopic analysis revealed localization to cell-cell contacts (i, arrowheads) and Weibel-Palade bodies (ii-iii, arrows). Scale bars, 100 nm. Images in (A) and (B) are representative of at least three independent experiments. (C) Immunogold labeling of resting human control platelets reveals APOLD1 localized to the membranes of α-granules (ii-iii) and to have an eccentric localization in the granule lumen, suggesting a possible association with VWF (iv). Of note, APOLD1 was not detected on the platelet surface. Scale bars, 200 nm (i) or 50 nm (ii-iv). Images are representative of one experiment.
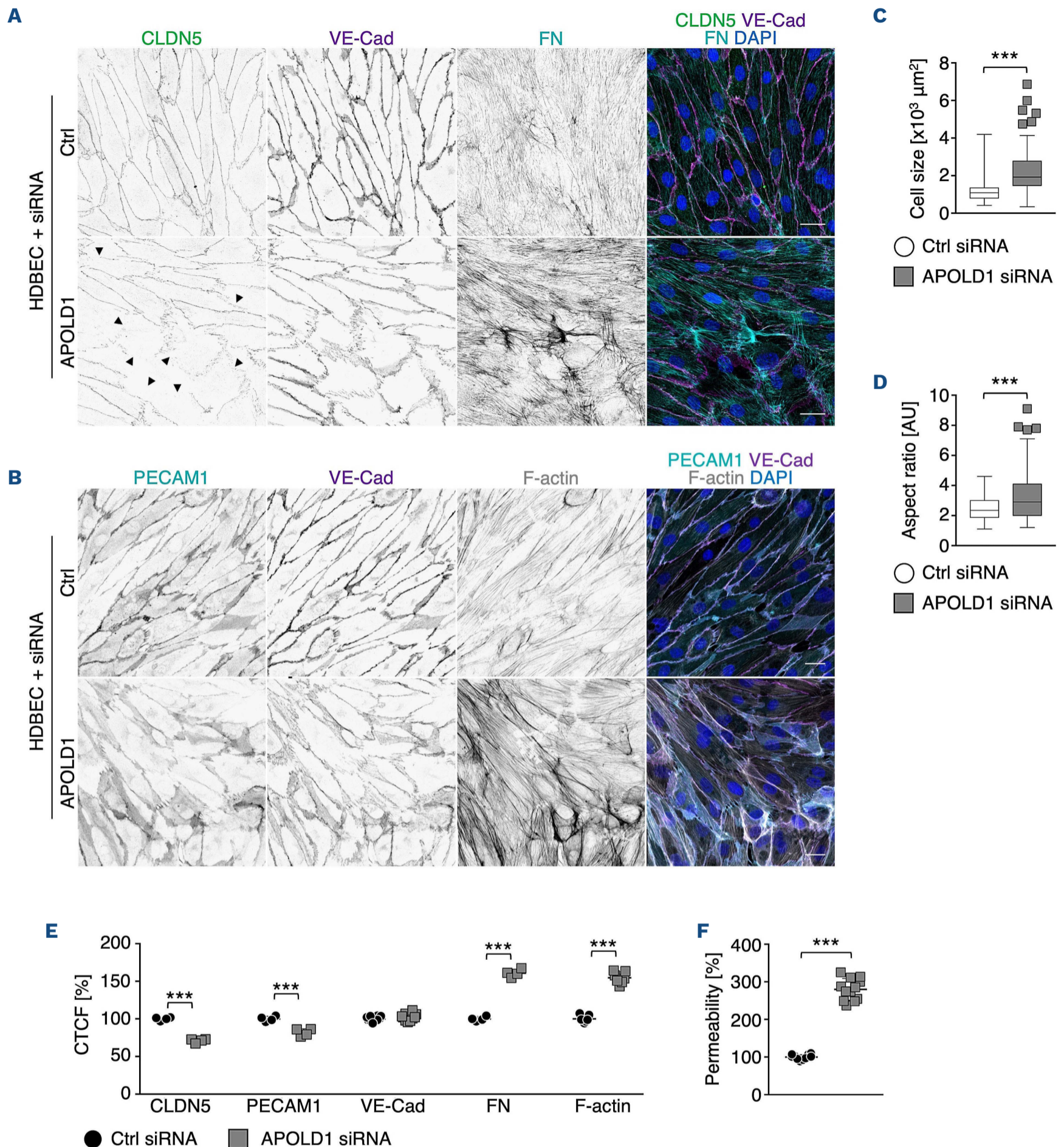
Figure 2. *APOLD1* silencing alters cytoskeletal and junctional organization of human dermal blood endothelial cells. (A, B) *APOLD1* silencing in human dermal blood endothelial cells (HDBEC) alters the organization of cell-cell junctions (claudin 5, CLDN5; vascular endothelial cadherin, VE-Cad; platelet-endothelial cell adhesion molecule 1, PECAM1/CD31) as well as cytoskeletal architecture and leads to increased fibronectin (FN) fibrillogenesis. Arrowheads in (A) highlight disrupted/CLDN5-negative junctions. Scale bars, 25 μm. Images are representative of three independent experiments. (C, D) Lack of APOLD1 results in increased HDBEC size and altered shape (aspect ratio = major axis:minor axis). Box plots display first and third quartiles, and whiskers mark minimum and maximum values unless exceeding 1.5 times the interquartile range of at least 150 cells per group from three independent experiments; symbols represent outliers, and the horizontal line denotes the median. (E) Image analysis revealed reduced immunolabeling intensities of the junctional proteins CLDN5 and PECAM1/CD31, alterations of VE-Cad distribution as well as enhanced FN fibrillogenesis and actin stress fiber formation, which is reminiscent of endothelial cell activation leading to increased (F) endothelial permeability (40 kDa dextran-FITC). Data in (E) represent the mean ± standard deviation. Each symbol in (E) represents the average of at least 100 cells from an individual experiment. Pooled data from at least four experiments are displayed. Each symbol in (F) represents one replicate from three independent experiments. Wilcoxon-Mann-Whitney test, ***P<0.001. CTCF: corrected total cell fluorescence.

EC junctions as well as cytoskeletal architecture and thereby in modulating endothelial permeability. Moreover, they suggest a critical threshold level of APOLD1 to maintain endothelial homeostasis.

APOLD1 interferes with the biology of endothelial cell storage organelles

We next further explored the implication of APOLD1 localization to endothelial WPB. To this end we took a closer look at VWF, a major constituent of WPB in EC and present in platelet α-granules.[16–19] Immunofluorescence labeling and immunoblotting revealed that *APOLD1*-silenced HDBEC in culture were almost devoid of VWF (Figure 3A, B). Changes in WPB content were not restricted to VWF but, significantly, were also associated with a reduction in cellular ANGPT2 (Figure 3A, B), confirming impaired storage.[20] In agreement, we found markedly elevated levels of VWF and ANGPT2 in the supernatant of *APOLD1* siRNA-treated HDBEC as compared with controls (Figure 3C, D), excluding impaired protein production as the cause. Using transmission electron microscopy, we readily observed WPB with the typical rod-shaped and striated ultrastructure in control cells (Figure 3E$_i$, F$_{i-ii}$). In contrast, we found that structurally abnormal organelles morphologically resembling autophagosomes with the typical isolation membrane predominated in *APOLD1* siRNA-treated HDBEC (Figure 3E$_{ii}$, F$_{iii}$). Immunogold labeling of VWF revealed that the remaining VWF in APOLD1-deficient HDBEC was mainly found in large vacuoles (Figure 3F$_{iii}$). An occasional WPB still labeling for VWF was seen apparently releasing its cargo into a vacuole (Figure 3F$_{iv}$). Notably, control cells were devoid of these vacuoles and labeling for VWF was restricted to WPB (Figure 3E$_{i-ii}$).
In summary these results suggest a role of APOLD1 in modulating endothelial WPB biology.

APOLD1 modulates Weibel-Palade body biology via secretory autophagy

Previous studies have identified a critical role of autophagy in WPB biogenesis and release.[21] Given the excessive WPB release from HDBEC in the absence of APOLD1 (Figure 3A-D), we speculated that loss of APOLD1 would interfere with autophagy flux and thereby affect the secretory pathway. An increased expression of the autophagy markers SQSTM1 and LC3B in *APOLD1* siRNA-treated HDBEC was indeed reminiscent of altered autophagy flux (Figure 4A-D). Furthermore, there was increased co-localization of VWF with LC3B and the late endosomal/autophagosomal marker RAB7, whereas the association with SQSTM1 and the lysosomal marker LAMP1 was decreased (Figure 4A-F, *Online Supplementary Figure S4*). This was accompanied by a decreased ratio of mature and pro-VWF in APOLD1-deficient HDBEC, revealing abnormal autophagy-dependent proteolytic processing (Figure 5A, B).

Significantly, blocking the fusion of autophagosomes with lysosomes, a final step of autophagy, with chloroquine resulted in an accumulation of lipidated LC3B-II and SQSTM1 in control HDEBC but did not affect the levels in *APOLD1*-silenced HDBEC (Figure 5A, C, D). All of these features have previously been associated with impaired autophagy flux likely in favor of increased priming of WPB for secretory autophagy.[21,22] Therefore, we next silenced *autophagy related 5* (*ATG5*) and *ATG7* genes which are critical for the initiation of autophagy and are implicated in WPB maturation as well as cargo release.[21] Strikingly, simultaneous loss of *ATG5* or *ATG7* with *APOLD1* partially restored the presence of WPB as compared with that in APOLD1-deficient HDBEC (*Online Supplementary Figure S5A-C*). Moreover, this led to a reduced release of WPB, evidenced by a decreased presence of VWF and ANGPT2 in the cell culture supernatant of *APOLD1/ATG5* and *APOLD1/ATG7* double-silenced HDBEC (*Online Supplementary Figure S5D-F*). These findings reveal a role of APOLD1 in regulating WPB release through modulation of autophagy flux and suggest secretory autophagy as the primary route for the excessive WPB cargo release in the absence of APOLD1.

APOLD1^{R49*} associates with bleeding and vascular problems in a family with an inherited disorder

Among the patients studied by the French Reference Center for Hemorrhagic Syndromes there was a large family with an inherited bleeding disorder for which, despite extensive investigations over many years on coagulation factors and platelet biology in several expert centers (*Online Supplementary Tables S1-S3*), no obvious cause could be identified. Based on these studies a vascular defect was suspected. The family history of the inherited bleeding disorder extends over three generations (Figure 6A). The index patients are two sisters (pedigree member [PM] 4 and PM6) (Figure 6A, *Online Supplementary Table S1*), now over 70 years old, who had a severe, atypical bleeding syndrome that was also present in their deceased father (PM1). In addition to the index patients, two of their children (PM9 and PM11), now adults, also suffer from excessive bleeding (Figure 6A, *Online Supplementary Table S1*). Their syndrome is characterized by severe spontaneous bleeding episodes during childhood, with extensive hemorrhage at menarche for the three affected women (PM4, PM6, PM9) which was difficult to control, and required hospitalization for PM9. Tranexamic acid was ineffective; different oral contraceptive therapies were tried for all of them but often not tolerated; PM9 recently received leuprorelin injections.
PM6 and PM9 have also experienced periods of gastrointestinal bleeding. For PM6, this occurred in her sixties and was intermittent but not abundant. For PM9, gastrointestinal bleeding was observed every 2-3 years during childhood but then stopped. Endoscopic investigations were not per-
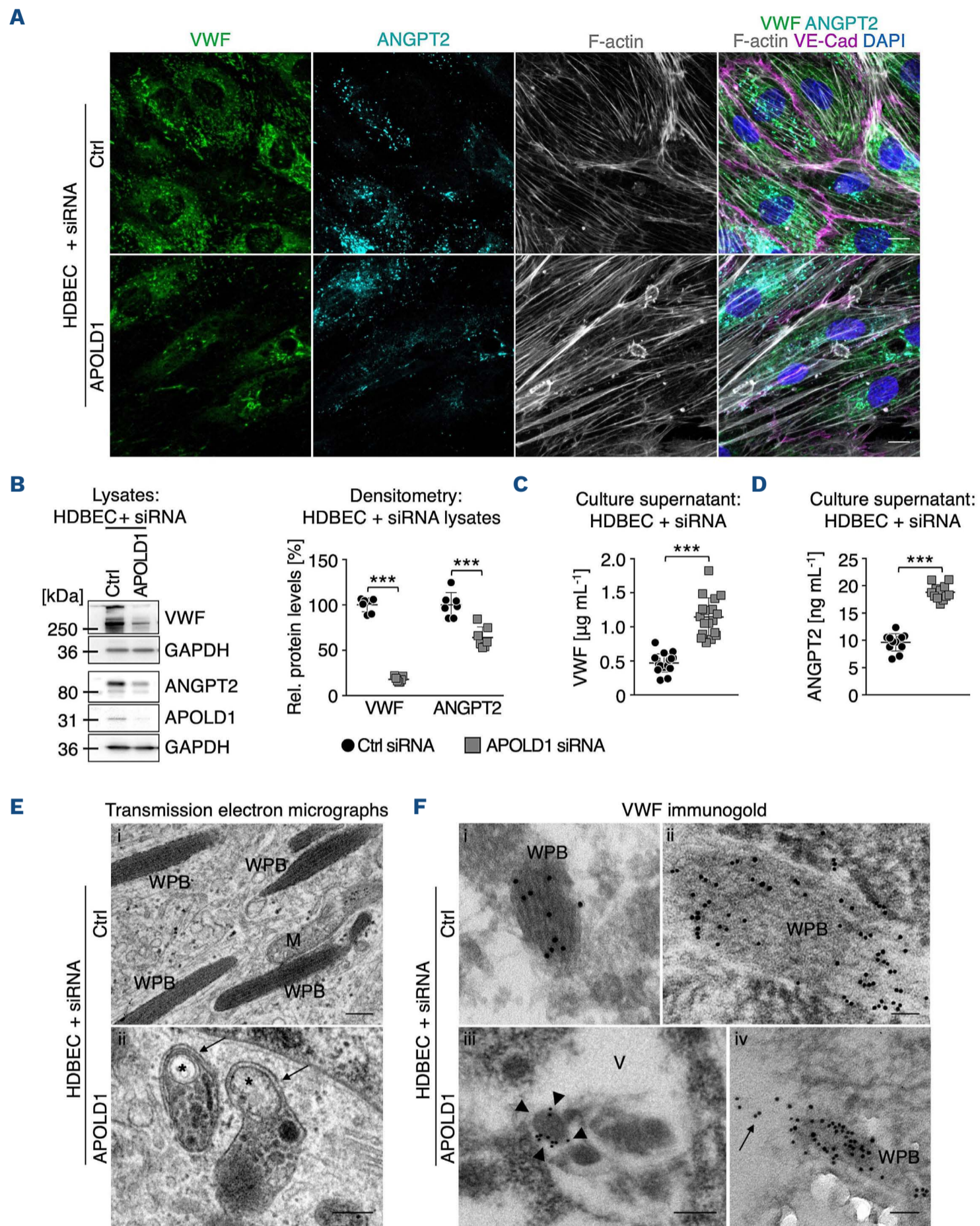
Figure 3. APOLD1 modulates Weibel-Palade body biology. (A-C) *APOLD1* silencing results in a loss of the major Weibel-Palade body (WPB) constituent von Willebrand factor (VWF) as well as angiopoietin 2 (ANGPT2) as revealed by (A) immunolabeling and (B) immunoblotting with subsequent densitometric quantification of VWF and ANGPT2 levels relative to GAPDH in total cell lysates of control and *APOLD1* siRNA-treated human dermal blood endothelial cells (HDBEC). Scale bars, 25 µm. Images and immunoblots are representative of at least three independent experiments. Each symbol in (B) represents one experiment and horizontal lines denote the mean ± standard deviation (SD). Wilcoxon-Mann-Whitney test, ***$P<0.001$. (C, D) VWF and ANGPT2 content in the supernatant of control and APOLD1 *siRNA*-treated HDBEC determined by enzyme-linked immunosorbent assay. Each symbol represents an individual sample and horizontal lines denote mean ± SD. Pooled data from four independent experiments are displayed. Wilcoxon-Mann-Whitney test, ***$P<0.001$. (E) Electron microscopic images of WPB in control siRNA-treated HDBEC (i) and autophagosomes (asterisks) with a developing isolation membrane (arrows) in *APOLD1*-silenced HDBEC (ii). M: mitochondria. Scale bars, 200 nm. Electron microscopic images are representative of three independent experiments. (F) Immunogold (5 or 10 nm gold particles) labeling of VWF highlights WPB with the typical striated rod-shaped structure in control cells (i-ii) while in *APOLD1*-silenced HDBEC (iii-v) VWF labeling was detected in vacuoles containing amorphous material (iii, arrowheads) and into which WPB release their cargoes (arrows in iv). Scale bars, 50 nm (i-ii, iv) or 100 nm (iii). Images are representative of three independent experiments.
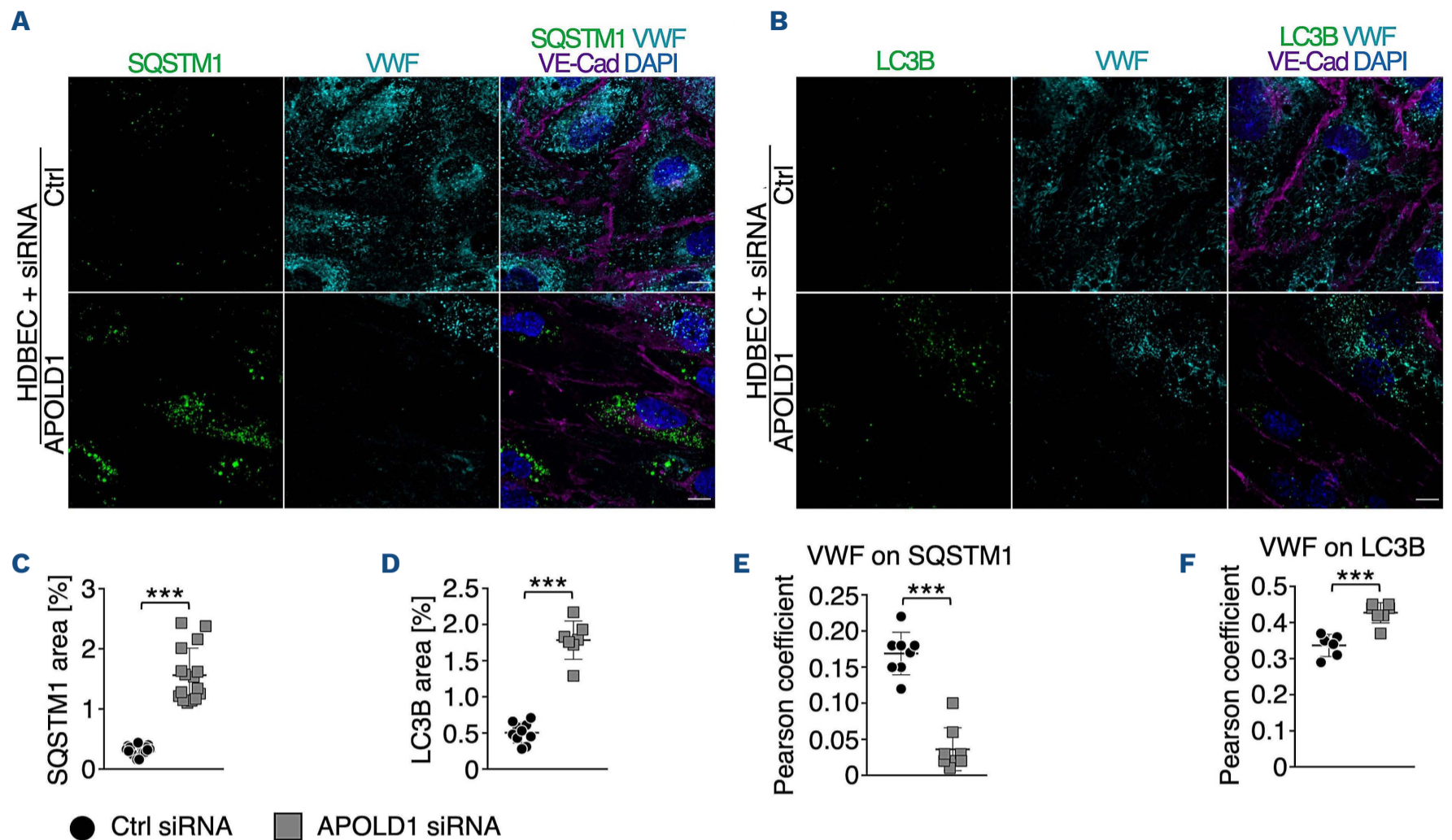
Figure 4. Increased release of Weibel-Palade bodies likely occurs via dysfunctional autophagy flux. (A-F) Immunolabeling and subsequent image analysis of control or *APOLD1* siRNA-treated human dermal blood endothelial cell (HDBEC) monolayers reveals increased expression of autophagy markers (A, C) SQSTM1 and (B, D) LC3B in the absence of APOLD1. Von Willebrand factor (VWF) co-localized to a lesser extent to (A, E) SQSTM1 but showed an increased localization to (B, F) LC3B-positive vesicles upon *APOLD1* silencing. Each symbol in (C-F) represents one analyzed (N≥6) image. Horizontal lines represent the mean ± standard deviation. Wilcoxon-Mann-Whitney test, ***P<0.001. Images are representative of at least three independent experiments. Scale bars, 10 μm.

formed so that the presence of mild angiodysplasia cannot be excluded. Surgery (PM4, PM6, PM9, PM11) and childbirth (PM4, PM9) was on occasion accompanied by dramatic blood loss and platelet transfusions were ineffective. For PM9 bleeding during delivery was severe and persisted despite continuous transfusions of numerous packed red blood cells and platelet concentrates, but then gradually ceased. Tubal ligation was performed immediately after her first delivery and for PM6 when she was 36 years old. Since middle age, no spontaneous bleeding has been observed for the patients. Another characteristic of the three female cases was the presence of microcirculatory problems (*Online Supplementary Table S1*). It is noteworthy that the use of vasodilators, piribedil (PM4, PM6) and dihydroergocristine (PM9), for the treatment of Raynaud syndrome or retinal ischemia as well as aspirin (PM6, PM11) intake aggravated the bleeding tendency. Conversely, the use of desmopressin to increase VWF secretion from EC in PM9 provoked a transiently impaired microcirculation evidenced by the appearance of livedo reticularis affecting her legs, due to which the treatment was discontinued (*Online Supplementary Table S1*).

Whole exome sequencing of DNA from PM4, PM6, PM9,

PM12 and PM13 identified a heterozygous nonsense c.145_146delinsTA; p.R49* variant in *APOLD1* predicted to generate a premature stop codon at the early position 49 (detailed in *Online Supplementary Information*). Interestingly, the nonsense stop-gain p.R49* variant results from a combination *in cis* of the common c.146G>A; p.R49Q (rs4763876; minor allele frequency 0.05292 Trans-Omics for Precision Medicine [TOPMed] and 0.07359 for the genome Aggregation Database [gnomAD]; predicted to be benign by Polyphen and tolerated by SIFT) and the rare missense c.145C>T; p.R49W (rs757476941; minor allele frequency 7.964×10^{-5} TOPMed and 6.637×10^{-5} for the gnomAD; predicted by Polyphen to be probably damaging and by SIFT as potentially deleterious) nucleotide substitution in *APOLD1* (Figure 6A, *Online Supplementary Figure S6*). Sanger sequencing of family members confirmed co-segregation of the R49* variant with the bleeding syndrome and additionally showed the presence of the common p.R49Q variant alone in asymptomatic relatives. Of note, PM4 was homozygous for the c.146G>A nucleotide substitution resulting in a compound heterozygous genotype of p.[R49Q];[R49*] (Figure 6A, *Online Supplementary Figure S6*). Except for the NM_006040:c.G1336T variant,
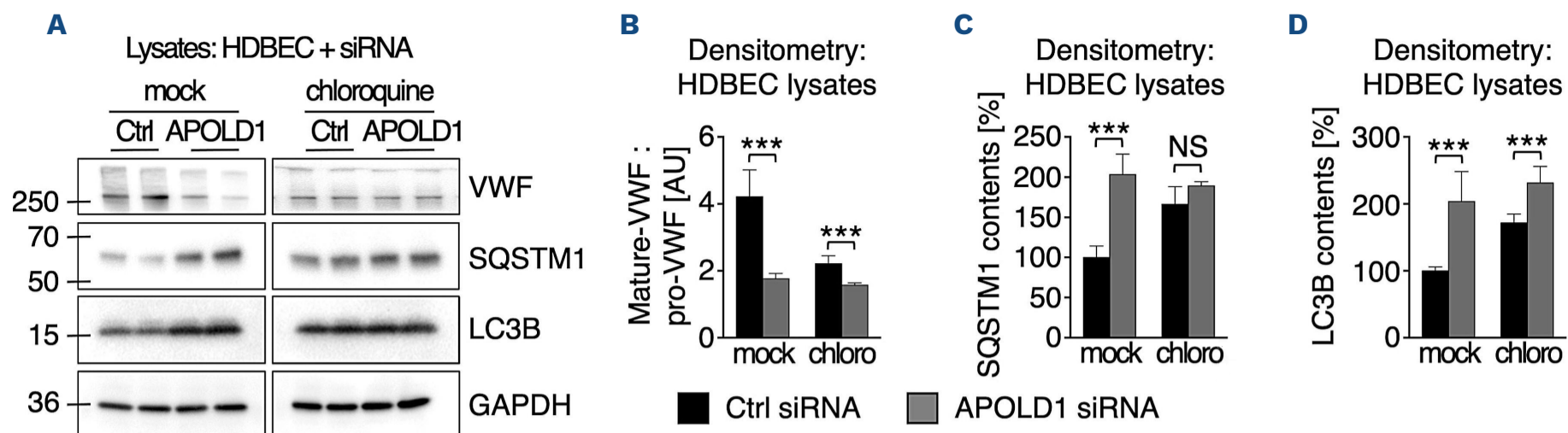
Figure 5. Impaired proteolytic processing of von Willebrand factor upon loss of APOLD1. (A) Immunoblotting of lysates from mock and chloroquine-treated (25 μM for 12 h) control or *APOLD1* siRNA-treated human dermal blood endothelial cells (HDBEC) with subsequent densitometric quantification of (B) proteolytic VWF processing, (C) SQSTM1 and (D) LC3B I/II expression. Immunoblots are representative of at least three independent experiments. Bar graphs in (B-D) represent the mean ± standard deviation. Two-way analysis of variance followed by the Sidak multiple comparison test, ***$P<0.001$.

which was not considered relevant on the basis of *HS3ST4* gene function, none of the other 17 candidate rare variants was predicted to be disease-causing, and no other candidate mutations were present in any gene known to be associated with an inherited platelet- or vascular-derived bleeding disorder (*Online Supplementary Table S4*). Of note, the whole exome sequencing covered coding and flanking regions that were scrutinized for the presence of single nucleotide variations and insertions/deletions. More complex structural variations, or variations outside coding or flanking regions are not included in whole exome sequencing analyses.

Immunofluorescence labeling and immunoblot analysis revealed an approximately 50% reduction of APOLD1 in platelets from PM4 and PM6 as compared to levels in healthy controls (Figure 6B, C), which is in agreement with the heterozygous transmission of the *APOLD1*[R49*] variant (Figure 6A). Interestingly, despite the decreased labeling of α-granules by anti-APOLD1 antibodies (Figure 6D), granule numbers were normal (Figure 6D, E). Significantly, a decreased α-granule VWF content was noted when comparing the number of α-granules positive for VWF and P-selectin (Figure 6D, F, *Online Supplementary Figure S7*). This observation parallels the above-identified role of APOLD1 in endothelial VWF biology. In addition, we observed plasma VWF values to be either increased or at the high normal range (VWF:Ag: 186% for PM4; 127% for PM6; 157% for PM9; 186% for PM11; normal range <150%). It should be noted that the blood group of all patients is A (*Online Supplementary Table S1*). In addition, ANGPT2 plasma levels (2231 pg/mL for PM4; 2490 pg/mL for PM6; 1935 pg/mL for PM11; normal range 1189±77 pg/mL) were increased in the patients studied, while the concentrations of endothelium-stabilizing ANGPT1 (1191 pg/mL for PM4; 1463 pg/mL for PM6; 1135 pg/mL for PM11; normal range 2893±457 pg/mL) were decreased (*Online Supplementary Table S2*).

These results suggest APOLD1 as a candidate gene for a novel EC-driven defect potentially underlying both the bleeding syndrome and microcirculatory problems in patients with an *APOLD1*[R49*] variant.

Discussion

Disintegration of the vascular barrier is a key feature of, and contributes to, the progression of various pathologies including cancer, chronic inflammatory conditions and cardiovascular diseases. Consequently, it is of much clinical interest to advance our understanding of the molecular machinery regulating endothelial integrity.[1,2,23] Our study identifies the immediate early gene *APOLD1* as a modulator of endothelial homeostasis, regulating the junctional-cytoskeletal interface crucial for endothelial permeability and WPB biology through secretory autophagy. In addition, we describe the co-inheritance of a c.145_146delinsTA variant in *APOLD1* leading to a premature stop codon at p.R49* that segregates to affected members of a family with an unusual bleeding diathesis. Based on their functions the other gene variants were not considered as candidates (*Online Supplementary Table S4*). Despite the reported expression of *APOLD1* in neurons,[12] there is no evidence of neurological abnormalities in affected patients, strongly suggesting a non-syndromic defect.

Our *in vitro* studies showed that APOLD1 localizes to HDBEC cell junctions and to WPB. Strikingly, loss of APOLD1 disrupted the cytoskeletal and junctional organization of HDBEC with loss of the major junctional components VE-Cad and claudin-5,[14] likely accounting for the increased vascular permeability and altered central function of the EC cytoskeleton. However, much remains to be learned of the role of the associated cytoskeleton in maintaining EC morphology, junctional integrity and dynamics, as well as its
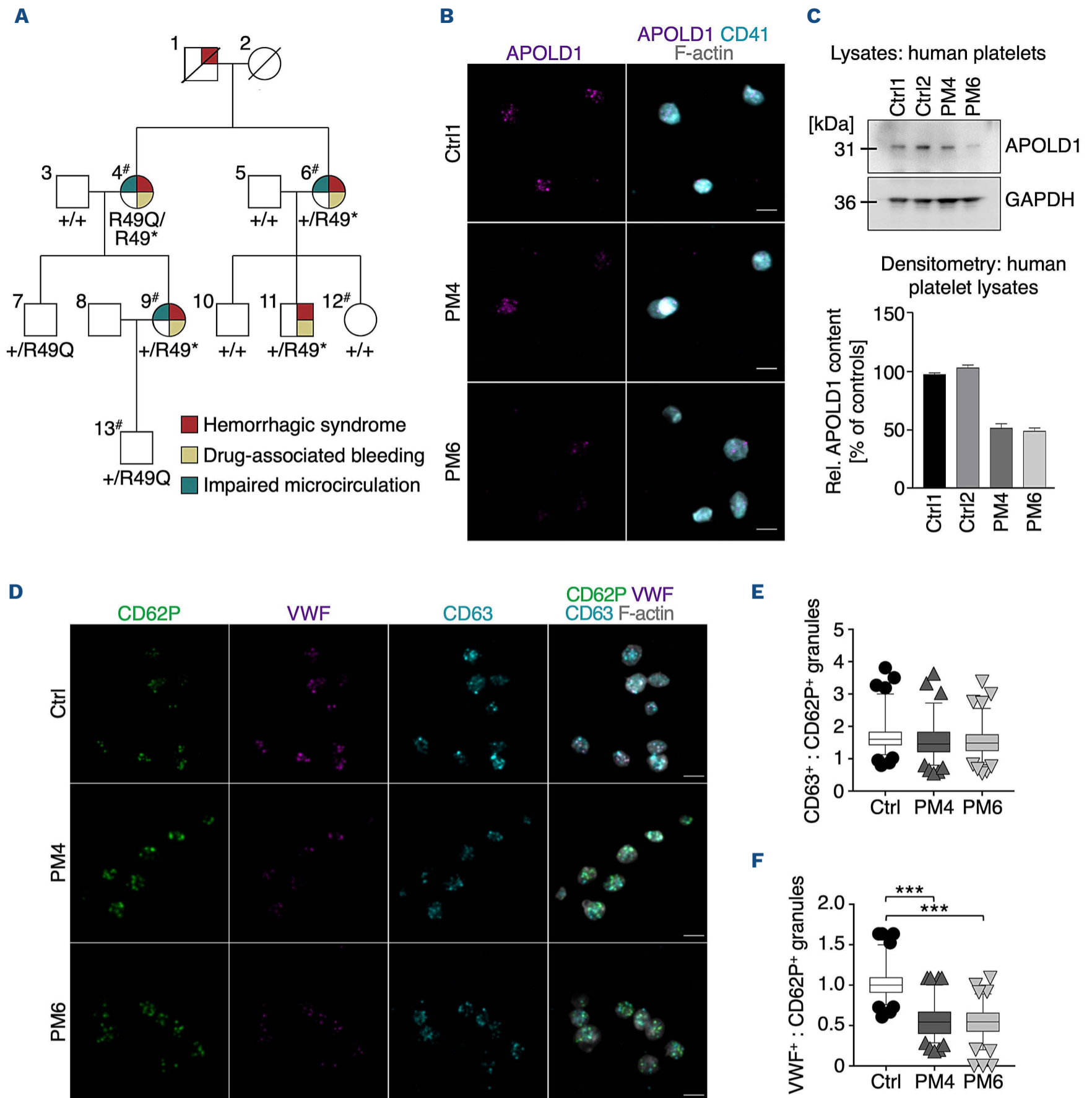
Figure 6. *APOLD1* is a candidate gene for a bleeding diathesis. (A) Pedigree of the family with a variant in *APOLD1*. The red filled symbols indicate a bleeding diathesis co-segregating with a nonsense c.145_146delinsTA variant in *APOLD1*, resulting in a premature stop codon at arginine 49 (R49*). Pedigree members (PM) 7 and 13 only carry the more frequent single base pair substitution c.G146A in *APOLD1* (R49Q) which was not associated with a bleeding syndrome. The hashtags indicate patients studied by whole exome sequencing. The other family members have been subjected to Sanger sequencing of *APOLD1*. Green filled symbols indicate occurrence of impaired microcirculation and yellow filled symbols of drug-associated bleeding. (B) Resting poly-L-lysine immobilized platelets from healthy control and PM4 and PM6 were stained for APOLD1 (magenta), CD41 (cyan) and F-actin (gray). Scale bars, 3 μm. (C) APOLD1 protein expression was analyzed by immunoblotting and densitometric quantification relative to GAPDH of platelet lysates from two unrelated healthy controls as well as PM4 and PM6. The antibody was directed against amino acids 139-192 and only detects full-length APOLD1. Immunoblots are representative of three experiments. Data represent the mean ± standard deviation (SD). (D) Resting platelets from controls or PM4 and PM6 were labeled for CD62 (P-selectin, green; α-granule marker), von Willebrand factor (VWF, magenta; α-granule marker), and CD63 (granulophysin, cyan; δ-granule/lysosome marker). F-actin is highlighted in gray. Scale bars, 3 μm. (E, F) Quantification of CD62P-, VWF- and CD63-positive granules per platelet from healthy controls, PM4 and PM6. Box plots display first and third quartiles, and whiskers mark minimum and maximum values unless exceeding 1.5 times the interquartile range of at least 100 cells per group; symbols represent outliers, and the horizontal line denotes the median. Results were analyzed by one-way analysis of variance followed by the Dunnett multiple comparisons test, ***$P<0.001$.

potentially cell type- and vascular bed-specific regulation.[24–28] *APOLD1* silencing also perturbed WPB biology with an increased release of cargoes including VWF and ANGPT2[17–20,29] due to impaired autophagy flux.[30] In support, biochemical and ultrastructural analyses revealed a reduced content in WPB, an abnormal presence of autophagosomes as well as the detection of VWF inside large vacuoles in *APOLD1* siRNA-treated HDBEC. A seminal study by Torisu *et al.* identified a critical role of autophagy flux and *ATG5* as well as *ATG7* for basal WPB release.[21] In our experiments the additive loss of *ATG5* or *ATG7* in *APOLD1*-silenced HDBEC partially restored the presence of WPB, confirming the participation of APOLD1 in the process of autophagic WPB secretion.[21,30] Globally, these results suggest the presence of a signaling cascade that regulates secretory autophagosome-trafficking of WPB and our results indicate that APOLD1 plays a central role therein.

Various cellular mechanisms can contribute to endothelial destabilization including kinase-/phosphatase-mediated phosphorylation/dephosphorylation of junctional proteins or Rho GTPase signaling and the associated cytoskeletal alterations.[23] Of note, ANGPT2 has previously been shown to cause destabilization of the endothelium, promote inflammation, and to bind directly to integrin α5β1 and activate it, thereby leading to junction dismantling.[4,31–34] Consequently, it is tempting to speculate that the excessive WPB release may directly contribute to the junctional and cytoskeletal alterations as well as to the increased endothelial permeability of *APOLD1*-deficient HDBEC. In support of this, we observed enhanced fibronectin fibrillogenesis of *APOLD1* siRNA-treated cells, a process that involves ligand competent integrin α5β1 in fibrillar adhesions.[34,35]

Interestingly, upregulation of *APOLD1* expression has been reported for patients under conditions of increased shear or cellular stress including inflammatory signals, physical exercise, and hypoxia.[36,37] Further studies will be required to understand the consequences of such modifications, including the activation of mechanosensory receptors and modifications of the vessel wall or WPB release. In an *APOLD1*-deficient mouse model, ischemic brain injury was evaluated because *APOLD1*, initially named *vascular early response gene* (*VERGE*), was recognized as an early gene expressed during ischemia.[9,11] Loss of *Apold1* did not affect the infarct volume of the induced stroke, but resulted in decreased neurogenesis and angiogenesis during the following month.[11] More recently, a mild prothrombotic phenotype was reported after laser-induced carotid vessel lesions in a similar model.[38] The mice had a somewhat shorter time to occlusion with increased tissue factor activity in the carotid artery and reduced phosphorylation of the signaling protein, AKT in aortae. Enhanced aggregation of washed platelets to collagen was noted in the absence of APOLD1. The platelet aggregation responses in our family using platelet-rich plasma showed no significant changes.

No data from additional models of thrombosis and hemostasis have been reported for A*pold1*^{-/-} mice. These published examples reflect the limited information available on the role of this gene and the consequences of its defects. Our *in vitro* studies in HDBEC showed an unexpected complex role of *APOLD1* in the regulation of vascular function and integrity through modulation of EC cytoskeleton and junctions as well as WPB biology. These findings expand the current understanding of APOLD1 function in EC. In the reported family with an unexplained complex phenotype combining severe bleeding and microvascular defects, whole exome sequencing, previously used to recognize new genes involved in unexplained inherited hematological disorders,[39–41] identified *APOLD1* as the first candidate gene for the affected patients. A premature *APOLD1*[R49*] stop codon variant arising from co-inheritance of a potentially deleterious missense variant c.145C>T; p.R49W and a single nucleotide polymorphism c.146G>A; p.R49Q co-segregated over three generations with a familial bleeding diathesis. This resulted in a truncated APOLD1 protein lacking the three transmembrane domains and the coiled-coil domain, which likely renders the protein dysfunctional. Importantly, the common c.146G>A; p.R49Q variant alone did not associate with a bleeding syndrome. In agreement with *APOLD1*[R49*] heterozygosity, we observed approximately 50% levels of full-length APOLD1 protein in platelets of PM4 and PM6. Furthermore, we found severe and progressive defects upon *APOLD1* silencing in primary HDBEC *in vitro*, suggesting a critical threshold level of APOLD1 to maintain normal EC physiology. A 50% reduction of APOLD1 in HDBEC significantly disrupted the cytoskeletal and junctional organization and affected WPB cargo content *in vitro*. This finding suggests that monoallelic defects of *APOLD1 in vivo* are compatible with a vascular defect. Of note, two other premature stop codon variants in *APOLD1* are present in the gnomAD database; however, their pathogenicity remains to be determined. It is important to note that disease-causing variants of MYH9-related disease, a well-studied bleeding disorder caused by rare monoallelic genetic variations, are also present in the gnomAD resource.[42]

The unusual familial vascular syndrome that was not accompanied by prolonged classical bleeding times, with the patients refractory to platelet transfusions argues against a platelet disorder. Moreover, bleeding was observed in response to the use of vasodilators (PM4, PM5, PM9) indicating an unusual vascular fragility. It therefore appears that the *APOLD1* defect in our patients affects critical aspects of the endothelium which favor the risk of hemorrhage, a process already described during inflammation,[43] and also observed in patients with hereditary hemorrhagic telangiectasia and cavernous malformations of the brain.[44,45] The increased plasma levels of VWF and ANGPT2 detected in the tested patients suggests that the excessive release of WPB identified *in vitro* for *APOLD1*-silenced HDBEC is also

present *in vivo*. In addition, the patients had decreased plasma levels of ANGPT1. This causes a change in the balance between ANGPT1 and ANGPT2 a situation known to impair EC integrity and vascular stability through tyrosine kinase Tie2/Tie1 signaling.[46] Changes in the ratio of both these ligands are associated with various pathological states including inflammation and sepsis.[43] Gastrointestinal bleeding is frequently present in von Willebrand disease as a result of reduced levels of VWF and increased ANGPT2 inducing proangiogenic dysplasia. The appearance of gastrointestinal bleeds in the described family with an *APOLD1[R49*]* variant raises questions on the underlying mechanisms and highlight the need for further investigations on the role of ANGPT1/ANGPT2 in the pathogenesis of lesion formation. The predicted abnormalities of WPB *in vivo* may contribute to the hemorrhagic syndrome during surgery. WPB defects are known to impair the local hemostatic response of the endothelium, even when plasma VWF levels are normal.[47,48] The observed irregular bleeding during various surgical interventions could also reflect the tissue-specific expression of *APOLD1* in different vascular beds (https://endotheliomics.shinyapps.io/ec_atlas/).[49] It is known that the placenta contains high amounts of APOLD1, possibly explaining the important bleeding observed during delivery (*v21.proteinatlas.org; www.proteinatlas.org/ENSG00000178878–APOLD1/tissue*).[50] The transiently perturbed microcirculation in PM9 after administration of desmopressin to increase endothelial VWF secretion for the prevention of her hemorrhagic syndrome further exemplifies the complexity of the phenotype of this family.

Beyond the classic forms of inherited bleeding disorder associated with a platelet abnormality or VWF defects, many patients with a family history of bleeding remain undiagnosed. To date, analyses of EC function are rarely performed, but should be considered in the future. To aid this, panels designed for high-throughput sequencing could integrate genes involved in EC interactions and WPB function.[51] We also anticipate that studies using patient-derived endothelial colony-forming cells, also referred to as blood outgrowth EC, will be useful to explore functional aspects of endothelial homeostasis and WPB biology for patients with an undiagnosed inherited bleeding disorder. Up to now most of the studies employing endothelial colony-forming cells have focused on patients with von Willebrand disease. Finally, an improved understanding of the critical levels of predominantly EC-derived ANGPT2, tissue plasminogen-activator and vascular endothelial growth factor for the maintenance of vascular homeostasis will help to understand the implications of EC in the pathogenesis of hemorrhagic syndromes.

In conclusion, we provide evidence that loss of APOLD1 results in increased endothelial permeability and modified EC function with an excessive release of WPB through secre-

tory autophagy. Our findings strongly suggest that APOLD1 modulates endothelial homeostasis with implications for vascular integrity and regulated WPB secretion. Given that *APOLD1* is an immediate early gene, its function might come into play fully only after traumatic vessel wall injury, or altered shear stress, for example, in the context of ischemia, atherosclerosis and inflammatory settings, which lead to a boost of *APOLD1* transcription.[9,36,37] Future studies with *Apold1^{-/-}* or knockin mice as well as patient-derived EC are required to define the role of APOLD1 in hemostasis more precisely and to further advance our understanding of the molecular functions of *APOLD1*.

Disclosures
No conflicts of interest to disclose.

Contributions
SS, PN and TM designed experiments and analyzed data; SS, JCB and MGB performed experiments; MR, MCA, DAT and MGB performed genetic studies; PN, ATN, JFS, MCA and MGB enrolled the patients and performed clinical and biological follow-up; SS, PN, ATN and TM wrote the manuscript with input from all the other authors.

Data-sharing statement
Data are available upon reasonable request.

References

1. Hu X, De Silva TM, Chen J, Faraci FM. Cerebral vascular disease and neurovascular injury in ischemic stroke. Circ Res. 2017;120(3):449-471.
2. Murakami M, Simons M. Regulation of vascular integrity. J Mol Med. 2009;87(6):571-582.
3. Bogatcheva NV, Garcia JGN, Verin AD. Molecular mechanisms of thrombin-induced endothelial cell permeability. Biochemistry (Mosc). 2002;67(1):75-84.
4. Hakanpaa L, Sipila T, Leppanen V-M, et al. Endothelial destabilization by angiopoietin-2 via integrin β1 activation. Nat Commun. 2015;6:5962.
5. Starke RD, Paschalaki KE, Dyer CEF, et al. Cellular and molecular basis of von Willebrand disease: studies on blood outgrowth endothelial cells. Blood. 2013;121(14):2773-2784.
6. de Boer S, Eikenboom J. Von Willebrand disease: from in vivo to in vitro disease models. Hemasphere. 2019;3(5):e297.
7. El-Mansi S, Nightingale TD. Emerging mechanisms to modulate VWF release from endothelial cells. Int J Biochem Cell Biol. 2021;131:105900.
8. Nagel T, Resnick N, Dewey CF, Gimbrone MA. Vascular endothelial cells respond to spatial gradients in fluid shear stress by enhanced activation of transcription factors. Arterioscler Thromb Vasc Biol. 1999;19(8):1825-1834.
9. Regard JB, Scheek S, Borbiev T, et al. Verge: a novel vascular early response gene. J Neurosci. 2004;24(16):4092-4103.
10. Liu F, Turtzo LC, Li J, et al. Loss of vascular early response gene reduces edema formation after experimental stroke. Exp Transl Stroke Med. 2012;4(1):12.
11. Mirza MA, Capozzi LA, Xu Y, McCullough LD, Liu F. Knockout of vascular early response gene worsens chronic stroke outcomes in neonatal mice. Brain Res Bull. 2013;98:111-121.
12. Koshimizu H, Matsuoka H, Nakajima Y, et al. Brain-derived neurotrophic factor predominantly regulates the expression of synapse-related genes in the striatum: insights from in vitro transcriptomics. Neuropsychopharmacol Rep. 2021;41(4):485-495.
13. Stritt S, Nurden P, Favier R, et al. Defects in TRPM7 channel function deregulate thrombopoiesis through altered cellular Mg(2+) homeostasis and cytoskeletal architecture. Nat Commun. 2016;7:11097.
14. Frye M, Dierkes M, Küppers V, et al. Interfering with VE-PTP stabilizes endothelial junctions in vivo via Tie-2 in the absence of VE-cadherin. J Exp Med. 2015;212(13):2267-2287.
15. Frye M, Taddei A, Dierkes C, et al. Matrix stiffness controls lymphatic vessel formation through regulation of a GATA2-dependent transcriptional program. Nat Commun. 2018;9(1):1511.
16. Cramer EM, Meyer D, le Menn R, Breton-Gorius J. Eccentric localization of von Willebrand factor in an internal structure of platelet alpha-granule resembling that of Weibel-Palade bodies. Blood. 1985;66(3):710-713.
17. Metcalf DJ, Nightingale TD, Zenner HL, Lui-Roberts WW, Cutler DF. Formation and function of Weibel-Palade bodies. J Cell Sci. 2008;121(Pt 1):19-27.
18. Rauch A, Wohner N, Christophe OD, et al. On the versatility of von Willebrand factor. Mediterr J Hematol Infect Dis. 2013;5(1):e2013046.
19. Randi AM, Smith KE, Castaman G. von Willebrand factor regulation of blood vessel formation. Blood. 2018;132(2):132-140.
20. Fiedler U, Scharpfenecker M, Koidl S, et al. The Tie-2 ligand angiopoietin-2 is stored in and rapidly released upon stimulation from endothelial cell Weibel-Palade bodies. Blood. 2004;103(11):4150-4156.
21. Torisu T, Torisu K, Lee IH, et al. Autophagy regulates endothelial cell processing, maturation and secretion of von Willebrand factor. Nat Med. 2013;19(10):1281-1287.
22. Wu Q, Hu Y, Jiang M, Wang F, Gong G. Effect of autophagy regulated by Sirt1/FoxO1 pathway on the release of factors promoting thrombosis from vascular endothelial cells. Int J Mol Sci. 2019;20(17):4132.
23. Claesson-Welsh L, Dejana E, McDonald DM. Permeability of the endothelial barrier: identifying and reconciling controversies. Trends Mol Med. 2021;27(4):314-331.
24. Cavey M, Lecuit T. Molecular bases of cell-cell junctions stability and dynamics. Cold Spring Harb Perspect Biol. 2009;1(5):a002998.
25. Tzima E, del Pozo MA, Shattil SJ, Chien S, Schwartz MA. Activation of integrins in endothelial cells by fluid shear stress mediates Rho-dependent cytoskeletal alignment. EMBO J. 2001;20(17):4639-4647.
26. García Ponce A, Citalán Madrid AF, Vargas Robles H, et al. Loss of cortactin causes endothelial barrier dysfunction via disturbed adrenomedullin secretion and actomyosin contractility. Sci Rep. 2016;6:29003.
27. Sauteur L, Krudewig A, Herwig L, et al. Cdh5/VE-cadherin promotes endothelial cell interface elongation via cortical actin polymerization during angiogenic sprouting. Cell Rep. 2014;9(2):504-513.
28. Stehbens S, Wittmann T. Targeting and transport: how microtubules control focal adhesion dynamics. J Cell Biol. 2012;198(4):481-489.
29. Spiel AO, Gilbert JC, Jilma B. von Willebrand factor in cardiovascular disease: focus on acute coronary syndromes. Circulation. 2008;117(11):1449-1459.
30. New J, Thomas SM. Autophagy-dependent secretion: mechanism, factors secreted, and disease implications. Autophagy. 2019;15(10):1682-1693.
31. Felcht M, Luck R, Schering A, et al. Angiopoietin-2 differentially regulates angiogenesis through TIE2 and integrin signaling. J Clin Invest. 2012;122(6):1991-2005.
32. Hakanpaa L, Kiss EA, Jacquemet G, et al. Targeting β1-integrin inhibits vascular leakage in endotoxemia. Proc Natl Acad Sci U S A. 2018;115(28):E6467-E6476.
33. Saharinen P, Eklund L, Alitalo K. Therapeutic targeting of the angiopoietin-TIE pathway. Nat Rev Drug Discov. 2017;16(9):635-661.
34. Clark K, Pankov R, Travis MA, et al. A specific alpha5beta1-integrin conformation promotes directional integrin translocation and fibronectin matrix formation. J Cell Sci. 2005;118(Pt 2):291-300.
35. Geiger B, Spatz JP, Bershadsky AD. Environmental sensing through focal adhesions. Nat Rev Mol Cell Biol. 2009;10(1):21-33.
36. Zhou L, Wang LM, Song HM, et al. Expression profiling analysis of hypoxic pulmonary disease. Genet Mol Res. 2013;12(4):4162-4170.
37. Simonsen ML, Alessio HM, White P, Newsom DL, Hagerman AE. Acute physical activity effects on cardiac gene expression. Exp Physiol. 2010;95(11):1071-1080.
38. Diaz-Cañestro C, Bonetti NR, Wüst P, et al. Apold1 deficiency associates with increased arterial thrombosis in vivo. Eur J Clin Invest. 2020;50(2):e13191.
39. Nurden AT, Nurden P. High-throughput sequencing for rapid diagnosis of inherited platelet disorders: a case for a European consensus. Haematologica. 2018;103(1):6-8.

40. Bastida JM, Lozano ML, Benito R, et al. Introducing high-throughput sequencing into mainstream genetic diagnosis practice in inherited platelet disorders. Haematologica. 2018;103(1):148-162.

41. Heremans J, Freson K. High-throughput sequencing for diagnosing platelet disorders: lessons learned from exploring the causes of bleeding disorders. Int J Lab Hematol. 2018;40(Suppl 1):89-96.

42. Bury L, Megy K, Stephens JC, et al. Next-generation sequencing for the diagnosis of MYH9-RD: predicting pathogenic variants. Hum Mutat. 2020;41(1):277-290.

43. Goerge T, Ho-Tin-Noe B, Carbo C, et al. Inflammation induces hemorrhage in thrombocytopenia. Blood. 2008;111(10):4958-4964.

44. Mallet C, Lamribet K, Giraud S, et al. Functional analysis of endoglin mutations from hereditary hemorrhagic telangiectasia type 1 patients reveals different mechanisms for endoglin loss of function. Hum Mol Genet. 2015;24(4):1142-1154.

45. Lopez-Ramirez MA, Pham A, Girard R, et al. Cerebral cavernous malformations form an anticoagulant vascular domain in humans and mice. Blood. 2019;133(3):193-204.

46. Bilimoria J, Singh H. The Angiopoietin ligands and Tie receptors: potential diagnostic biomarkers of vascular disease. J Recept Signal Transduct Res. 2019;39(3):187-193.

47. James AH, Eikenboom J, Federici AB. State of the art: von Willebrand disease. Haemophilia. 2016;22(Suppl 5):54-59.

48. Schillemans M, Kat M, Westeneng J, et al. Alternative trafficking of Weibel-Palade body proteins in CRISPR/Cas9-engineered von Willebrand factor-deficient blood outgrowth endothelial cells. Res Pract Thromb Haemost. 2019;3(4):718-732.

49. Kalucka J, de Rooij LPMH, Goveia J, et al. Single-cell transcriptome atlas of murine endothelial cells. Cell. 2020;180(4):764-779.e20.

50. Uhlén M, Fagerberg L, Hallström BM, et al. Proteomics. Tissue-based map of the human proteome. Science. 2015;347(6220):1260419.

51. Kat M, Margadant C, Voorberg J, Bierings R. Dispatch and delivery at the ER-Golgi interface: how endothelial cells tune their hemostatic response. FEBS J. 2022;289(22):6863-6870.

52. Gustafsson N, Culley S, Ashdown G, et al. Fast live-cell conventional fluorophore nanoscopy with ImageJ through super-resolution radial fluctuations. Nat Commun. 2016;7:12471.